Journal of Thermal Analysis, Vol. 36 (1990) 765-789

SINGLE RUN HEAT CAPACITY MEASUREMENTS

*Y. Jin** and *B. Wunderlich*

DEPARTMENT OF CHEMISTRY, UNIVERSITY OF TENNESSEE, KNOXVILLE, TN
37996-1600 AND CHEMISTRY DIVISION, OAK RIDGE NATIONAL LABORATORY, OAK
RIDGE, TN 37831-6197, USA

(Received July 5, 1989)

A study of single-run differential scanning calorimetry is presented considering baseline repeatability, crosstalk between the calorimeters, positioning of calorimeters, heating rate, sample mass, environment changes, sample pan mass, purge gas flow, instrument lags, and differences in heating rate between the calorimeters. The instrument considered was the du-Pont dual sample differential scanning calorimeter. The major errors are caused by environmental changes. All other errors seem to limit accuracy to ±0.3%, a very respectable level. After optimizing all parameters, heat capacities of aluminum, sodium chloride, quartz, polystyrene and selenium were measured between 348 and 548 K. The root mean square error of all measurements on comparison with well established adiabatic calorimetry is ±0.8%. This proves that single-run differential scanning calorimetry is possible, as predicted before, and improvements can still be made.

The improvement of measurement of heat capacity by differential scanning calorimetry (DSC) is one of the goals in our *ATHAS* laboratory. In the past, comparisons between various DSC's were made in high [1] and low temperature ranges [2], direct computerization was pioneered [3] and a data treatment method was developed that led in the Advanced THermal Analysis System (*ATHAS*) [4].

In all prior DSC measurements it was necessary to carry out three successive runs: 1. with both calorimeters empty to establish the zero; 2. with one calorimeter empty and one filled with sapphire (Al_2O_3) as standard sample; and 3. with one calorimeter empty and one filled with the unknown sample. These triple measurements take extra effort to get heat capacity data out of differential heat-flow information.

---

*On leave from the Dept. of Material Science, Fudan University, Shanghai, China

John Wiley & Sons, Limited, Chichester
Akadémiai Kiadó, Budapest

Besides the effort, such measurements also carry the problem of greater chance of systematic error. In case the overall thermal steady-state environment of the instrument changes during the course of the three successive measurements, all measurements must be repeated. It will be shown in this paper that such environmental effects are, indeed, the dominant error source.

In a previous paper [5] we speculated about a new method, called single-run DSC for heat capacity measurement, and developed the necessary mathematical background. In this paper, the first experimental results will be presented and some general experience and error analyses are given for the temperature range of about 320 to 570 K.

Measurements were made with the duPont 2100 Thermal Analyzer System with a 912 Dual Sample Differential Scanning Calorimetry (DSDSC) cell, governed by an Auto Sampler (AS). The following effects were studied: baseline repeatability; asymmetry of the calorimeters; sample placement; crosstalk between calorimeters; cell constant; temperature lag; effects of the temperature of the environment and the influence of the nitrogen gas flow; and the effect of heating rate differences between sample and reference.

From the repeatability of the results we conclude that it is possible to reach similar precision as with triple-run standard DSC and hope that with further improvements the precision may be increased. The major problem areas were identified and suggestions are given for their resolution so that it may be possible in the future to approach routine ±0.1% heat capacity measurements.

Experimental

Instrumentation

A commercially available duPont 2100 Thermal Analyzer System with a 912 Dual Sample DSC (DSDSC) and DSC Autosampler (AS) were used for thermal analysis of all samples. The instrument was controlled by an IBM Personal System/2 Model 60 computer (3MB RAM) with color monitor, IBM Proprinter II, 8 pen HP ColorPro Graphics Plotter and 3 disk-drives: A Winchester hard disk-drive (44 MB), a 3 1/2" floppy disk-drive (1.44 MB) and a 5 1/4" floppy disk-drive (365 KB). The computer is used either under MS-DOS 3.3 for general computation or the duPont TA System for thermal analysis. Under the TA system the number of files of the hard disks can be as much as 4,000 (depending on file size, governed largely by the sampling interval, set from a low of 0.2 s/point to a high of 50 s/point). The analog output of the DSC is converted to digital format by a voltage-to-frequency converter which effectively averages the full sampling interval. No further statistical averaging of data should thus be needed. For heat capacities that vary little with temperature it is thus sufficient to use the standard intervals of the *ATHAS* data bank for tabular representations (10 K intervals from 30 K to the upper limit of measurements).

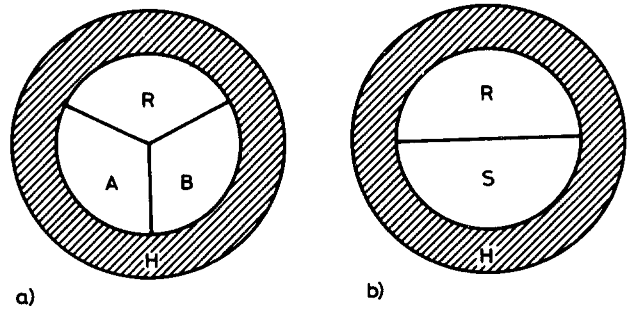

Fig. 1 Schematic of DSC cell, H: heater block; R: reference; and A, B, and S: samples (a) Dual Sample DSC (b) Normal DSC

Figure 1 is a schematic of the DSDSC cell in comparison to the normal DSC cell. Both of them need an empty pan on R, the reference position. For DSDSC, two samples, one placed on A and one on B, can be measured at the same time with the same thermal environment. This is not only of advantage because of the saving of time, it also reduces systematic experimental errors. The DSC Autosampler can save time, because it loads and unloads samples automatically, and then operates continuously according to the programmed run sequences. Up to 62 samples (including empty pans) can be loaded and set in up to 43 run sequences. Two other advantages of the DSC Autosampler are that the robot can minimize the sample placement error to within ±0.2 mm and it permits the use of the DSC during the night and week-end hours when environmental changes in temperature are minimized.

Before measurements, DSDSC was adjusted by hardware changes for control of temperature to within ±0.1 K, heat flow signal zero to lie between 0 to -0.5 mW and the baseline drift to be less than 0.1 mW from room temperature to 570 K. The adjustment of baseline-drift by instrument calibration is preliminary since full use of mathematical data analysis will in the future need uncorrected baselines [5]. Sample-temperature and heat-flow-signal zero can also be further adjusted by software, if necessary.

Indium was used as temperature and preliminary latent heat calibration standard. (Melting temperature = 429.8 K and heat of fusion 28.42 J/g). Sapphire (Al_2O_3) was used as final heat capacity calibration standard. All samples were encapsulated in standard aluminum pans (hermetically sealed pans).

All mass determinations were carried out on a Cahn electrobalance with a sensitivity of 0.01 mg and an overall accuracy of better than ±0.1%. Nitrogen gas was purged through the DSC cell at 10 ml/min.

For temperature calibration and cell constant evaluation, the latter being proportional to the latent heat, an indium sample was measured at different heating rates (1, 5, 10, 20 and 40 K/min). These data were collected with a sampling interval of 0.6 s/point and stored on hard disk for further analysis.

For heat capacity measurements, one standard sapphire, one unknown sample, and one empty pan were placed on A, B, and R, respectively. All pan weights were adjusted to within ±0.1 mg. Symmetry was also checked by running three empty pans. A typical DSC was run and consisted of the following: 1. an initial isothermal section; 2. a period of linearly programmed heating, the actual measurement, and 3. a final isotherm. (For example, an initial isothermal of 3 minutes at 350 K, heating at 10 K/min to 560 K, and then, a final isothermal 5 minutes at 560 K). Data were stored on disk with a

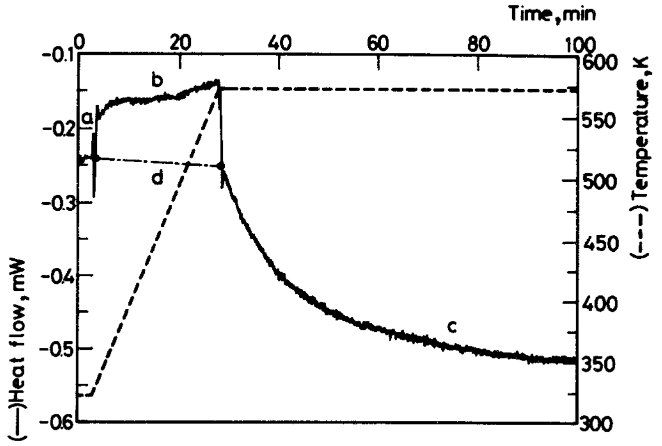

Fig. 2 A typical example in a time-based graph of heat capacity measurement. (a) Starting isotherm; (b) Linear programmed heating; (c) Ending isotherm; (d) The extrapolated isotherm between starting and ending isotherm

sampling interval of 3.0 s/point. The heat capacity calculations were done from the recorded amplitudes. Figure 2 shows a typical example in a time-based graph for three empty pans: a) is the initial isotherm, b) the linear programmed heating portion, c) the final isotherm, d) the broken line from the end of a) to the beginning of c) is the extrapolation between the initial and the final isotherms. In the example of Fig. 2 the final isothermal baseline recording was extended to very long times to check on the drift of the instrument. Obviously it takes a long time to reach a new steady state, so that the measurement is quite dynamic and the baseline cannot be set at overall steady state. The change in isotherm must be part of the calibration.

Materials used

A sapphire disk and indium were supplied with the accessory kits of the DSC instruments. In addition, granular sapphire traced to the original calorimetry of diameter about 1 mm was supplied by NBS, Gaithersburg, MD. Aluminum and selenium pellets of 99.999% purity were obtained from Aldrich Chem. Co., Milwaukee, WI. Sodium chloride of analytical reagent grade was acquired from Mallinckrodt Co., Paris, KY. A standard sample of polystyrene of MW = 100,000, $M_w/M_n < 1.06$ was bought from Polyscience Inc., Warrington, PA. The quartz used in this work was pure, supplied by the University glassblower in suitable shape.

Results and discussions

A. Adjustment of the Instrument

Before measurement of heat capacity, the instrument was adjusted to the most reproducible condition. A check was made of the Dual Sample DSC and the Autosampler. The former is the basic requirement for single run heat capacity measurements. The latter can minimize the error in sample placement, as well as permit automatic and continuous experiments.

1. Baseline repeatability of the dual sample DSC

Three empty aluminum pans were placed on positions R, A, and B, (Fig. 1). The DSC was then run as follows: fast heating from room temperature to 358 K, initial isotherm of 3 minutes at 358 K, programmed heating at 10 K/min to 558 K, final isotherm of 5 minutes at 558 K. This was followed by uncontrolled cooling to 358 K, and nine times repetition of the run. The

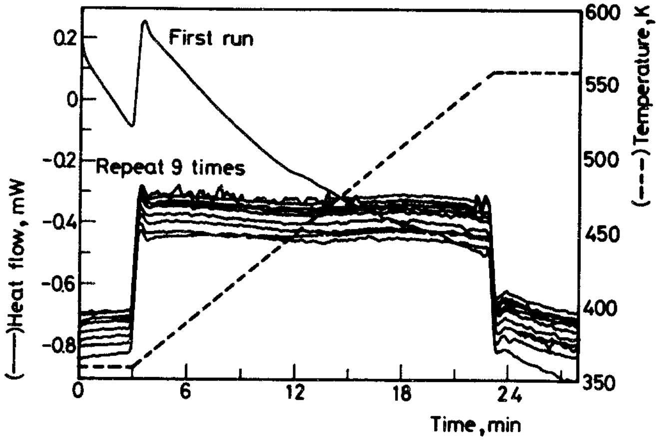

Fig. 3 Baseline repeatability of cell A

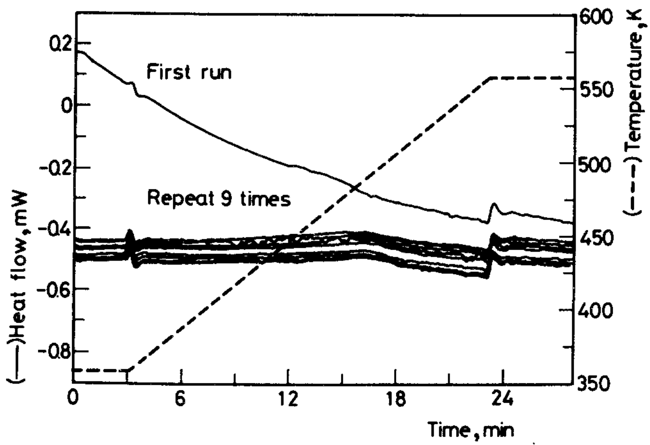

Fig. 4 Baseline repeatability of cell B

results are displayed in Figs 3 and 4. The measured heat flow must be compared to a typical measurement with amplitudes of 10 to 20 mW. Figures 3 and 4 show that the recorded heat-flow amplitudes of the programmed heating change significantly in going from the first to subsequent runs. In fact, this first run error may account for many poor data in the literature. Excluding the first run, the recordings showed a maximum deviation of ±0.09 mW for cell A and ±0.05 mW for B. The corrected heat-flow amplitudes vary even less. They are determined by subtracting the extrapolated, isothermal baseline from the amplitude of the programmed heating (see Fig. 2). The measured fluctuations were ±0.010 mW for cell A and ±0.005 mW for B, about one tenth of the absolute fluctuation between successive runs. If the amplitude of an unknown sample were 10 mW, the baseline error would be only about 0.10% when determined in this fashion.

The much higher deviation of the first run underscores the importance of a similar thermal history of the instrument for a high quality heat capacity measurement. The Autosampler of the DSC has already a jacket-heater, surrounding the DSC cells and keeping the outside of the DSC cell at about 323 K. Such isolation from the environment is helpful to establish a reproducible thermal history, but additional insulation of the whole DSC and close temperature-control of the room with an effort to exclude drafts could improve the performance even further.

2. *Single-run heat capacity measurement*

For some initial single-run heat capacity measurements the heat capacity at a selected temperature was calculated using Eq. (1) which was derived for the assumption that $\mathrm{d}\Delta T_s/\mathrm{d}T_s$ and $\mathrm{d}\Delta T_r/\mathrm{d}T_r = 0$ [5]:

$$C_{pU} = C_{pS}(W_S/W_U)(A_U^B - A_E^B)/(A_S^A - A_E^A) \tag{1}$$

where C_p represents the heat capacities, W the masses and A the corrected heat flow amplitudes, the subscripts E, S, and U represent the empty, standard (sapphire) and unknown (to be measured) sample, respectively; and superscripts A and B represent cells A and B, respectively. Improvements on this simplest approximation will be considered in stages, as the reproducibility of the instrument is checked. If cell A and B were fully symmetric, the corrected heat flow amplitudes for the same, empty aluminum pans (A_E^A and A_E^B) should be identical and

$$C_{pU} = C_{pS}(W_S/W_U)(A_U^B/A_S^A) \tag{2}$$

and the heat capacity could then be measured by a single-run Dual Sample DSC without correction of asymmetry.

We selected a pair of sapphire samples of almost equal masses and three close to identical mass aluminum pans to carry out single-run heat capacity measurements based on the approximate Eq. (2), similar recordings as shown in Fig. (2) result from cells A and B. Table 1 gives the data. Column A lists the standard data for sapphire [9] and column C_p^B was calculated by Eq. (2). The difference between the heat capacities is 8 to 10%, caused largely by asymmetry between cells A and B. Without *any* calibration it is thus possible to make single-run heat capacity measurements with an estimated precision of 10%, and with an easy possibility of correction to higher precision using an asymmetry factor.

Table 1 First single-run heat capacity measurement on sapphire

T, K	C_p^A, J/K mol	C_p^B, J/K mol	Deviation, %
373.15	92.52	12.16	10.42
398.15	95.93	105.83	10.32
423.15	98.90	108.06	9.26
448.15	101.51	110.52	8.88
473.15	103.82	112.86	8.71
498.15	105.90	115.28	8.86
523.15	107.77	117.42	8.95
548.15	109.47	118.96	8.67

C_p^B was calculated by Eq. (2) on heating rate: 10 deg/min, gas flow rate: 10 ml/min, W_S = 62.64 mg, W_U = 62.38 mg

3. Symmetry of cells A and B

Comparing the baseline amplitudes of cell A in Fig. 3 and cell B in Fig. 4, the corrected heat flow amplitude of cell B is close to zero (less than 0.1 mW), but that of cell A is about 0.4 mW, i.e. the baseline of cell A is 0.5 mW higher than that of cell B. If one assumes the corrected heat flow amplitude of a sample to be 10 mW, the data of the sample on cell B will then be higher by about 5% than those on cell A because of asymmetry. A fact born-out by the data in Table 1.

Comparing the baseline repeatability of cells A and B from Figs 3 and 4, the fluctuations of cell A are almost twice that of cell B. Analyzing a second cell in our possession showed similar differences between the two sample positions. To reduce the influence of the difference in performance of position A and B, we decided to place the fixed sapphire standard on the poor-performance position, since other effects, such as sample placement, pan mass etc., which will be discussed below, are a minimum for the pan which is kept permanently on the same position.

To check on the symmetry of measurement of latent heat effects, the fusion of two indium samples was analyzed (Indium-1 and Indium-2). The samples masses were 9.865 mg and 9.645 mg, and the heating rate, 10 K/min. The range of measurement was from 413 K to 443 K. The measurement was followed by an exchange of Indium-1 and Indium-2 by the Autosampler and a repeat run. The overall measurement was then repeated twice. The melting point (T_m) and the enthalpy of fusion (ΔH_m) were calculated with the commercial software. The results are shown in Table 2. Comparing the same sample (Indium-1 or Indium-2) on cells A and B gives good agreement. This result indicates that the difference between cell A and B for temperature and cell constant is small.

4. *Effect of sample pan position*

We tested next the effect of pan position on the baseline repeatability.

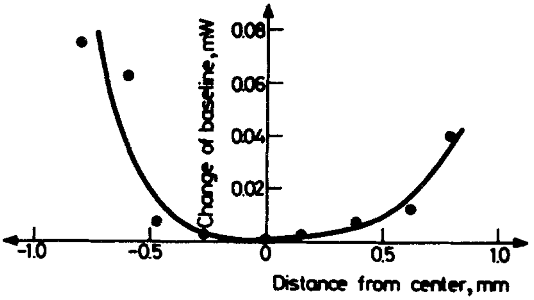

Fig. 5 Effect of sample pan position on baseline

Figure 5 shows the change in baseline, expressed by the corrected heat flow amplitude of an empty pan, with pan position. If the sample pan deviates from the center by less than 0.5 mm, the change of baseline is less than 0.01 mW for cell B. Only if the deviation of the pan position from the center is more than 0.5 mm, will there be a significant effect on the baseline. The Autosampler has a maximum error of ±0.2 mm, [6] i.e. it can reach the required ±0.5 mm repeatability easily.

Table 2 Comparison between cell *A* and *B* of the dual sample DSC. Measurement of melting temperature and heat fusion of indium

Sample	Cell	T_m, K /ΔH_m, J/g			
		First	Second	Third	Average
Indium-1*	*A*	429.67/24.00	429.65/24.04	429.65/24.03	429.66±0.01/24.02±0.02
Indium-1	*B*	429.70/24.16	429.66/24.10	429.63/24.15	429.66±0.04/24.14±0.02
Indium-2#	*A*	429.74/24.11	429.69/24.11	429.66/24.10	429.70±0.04/24.11±0.01
Indium-2	*B*	429.71/24.17	429.72/24.16	429.69/24.20	429.71±0.02/24.18±0.02

Indium-1*: 9.865 mg indium in a 26.44 mg aluminium pan,

Indium-2#: 9.645 mg indium in a 26.63 mg aluminium pan.

5. Effects of heating rate and sample mass

5.1 Crosstalk between dual sample cells

One of the assumptions made in describing a single-run DSC [5] was that there is no crosstalk between cells *A* and *B*, i.e. that endothermic or exothermic effects that occur in one cell only, do not contribute to the recorded amplitude in the other cell. To study crosstalk, one indium sample in the standard aluminum pan was placed on cell *A*, an equivalent, empty aluminum pan on cell *B*.

Table 3A Crosstalk from cell *A* to cell *B*

Heating rate, deg/min	Indium mass, mg					
	1.03	2.70	4.40	9.19	20.40	46.30
			ΔH_E, mJ on cell *B*			
1	0.0839	–0.0644	0.1016	0.2438	–0.0744	––0.0827
5	0.0240	0.0439	–0.0663	–0.0634	–0.0430	–0.2151
10	0.0114	–0.0381	0.0114	–0.0147	–0.1110	–0.2616
20	0.1072	0.0490	–0.0029	–0.0710	–0.0898	–0.1880
40	0.1673	–0.0748	0.1716	0.0823	0.1018	–0.0106
			ΔH_S, mJ on cell *A*			
1	28.10	71.15	109.65	226.53	486.13	1114.64
5	27.57	71.20	109.56	225.98	488.38	1113.05
10	27.50	71.25	109.65	226.17	489.19	1113.05
20	27.60	71.25	109.69	226.17	490.21	1114.44
40	29.05	72.28	109.96	226.63	488.58	1114.44
			Crosstalk, % = $100 \times \Delta H_E / \Delta H_S$			
1	0.30	0.09	0.09	0.11	–0.02	–0.01
5	0.09	0.06	–0.06	–0.03	–0.01	–0.02
10	0.04	–0.05	0.01	–0.01	–0.02	–0.02
20	0.39	0.07	–0.00	–0.03	–0.02	–0.02
40	0.58	–0.10	0.16	0.04	0.02	–0.00

Table 3B Crosstalk from cell *B* to cell *A*

Heating rate deg/min	Indium mass, mg					
	1.03	2.70	4.40	9.19	20.40	46.30
			ΔH_E, mJ on cell *A*			
1	–0.1373	0.0232	0.2553	–0.2887	0.0339	0.0186
5	–0.1465	–0.0562	–0.0232	–0.1412	–0.1424	–0.3011
10	–0.1331	–0.0673	0.0395	–0.0439	–0.1659	–0.1827
20	0.1012	0.0340	0.0964	–0.0047	–0.1004	–0.1976
40	–0.0793	–0.0106	0.0325	–0.0947	–0.2093	–0.0106
			ΔH_S, mJ on cell *B*			
1	27.35	70.12	107.32	228.56	499.60	1126.02
5	27.18	70.28	107.05	227.82	499.39	1123.24
10	27.13	70.25	107.18	228.00	500.00	1123.70
20	27.11	70.31	107.27	228.10	500.00	1125.09
40	27.55	70.82	107.54	228.92	501.02	1125.55
			Crosstalk, % = $100 \times \Delta H_E / \Delta H_S$			
1	–0.50	0.09	0.24	–0.13	0.01	0.00
5	–0.54	–0.08	–0.02	–0.06	–0.03	–0.03
10	–0.49	–0.10	0.04	–0.02	–0.03	–0.02
20	0.37	0.05	0.09	–0.00	–0.02	–0.02
40	–0.29	–0.01	0.03	–0.04	–0.04	–0.00

Then a run was made from 413 to 453 K at 10 deg/min. The crosstalk is then defined as:

$$\text{Crosstalk}_{A \rightarrow B}\ (\%) = \Delta H_E^B / \Delta H_S^A \times 100 \tag{3}$$

where ΔH_E^B and ΔH_S^A are the peak areas of the empty pan on cell *B* and the indium sample with aluminum pan on cell *B*, respectively. Both areas are calculated from the same experiment over the same temperature range. On exchanging *A* and *B*, ΔH_E^A and ΔH_S^B are measured for the analogous calculation of the crosstalk$_{B \rightarrow A}$ (%). Tables 3 and 4 show some results for different indium weights at different heating rates. The crosstalk between the two cells in either direction is negligible for heating rates of 5-20 K/min and indium weights of 3-45 mg. The computed data for ΔH_E show practically only random fluctuations, so that on recalculation per mg of indium, the runs

Table 4 Cell constants for cell (A/B)

Heating rate, deg/min	Indium mass, mg				
	0.632	2.696	7.242	10.820	18.570
1	1.163	1.126	1.114	1.100	1.091
	1.158	1.130	1.104	1.116	1.116
5	1.117	1.123	1.108	1.099	1.092
	1.149	1.133	1.105	1.117	1.116
10	1.126	1.124	1.108	1.098	1.092
	1.147	1.131	1.106	1.115	1.116
20	1.129	1.124	1.106	1.098	1.092
	1.154	1.131	1.105	1.115	1.116
40	1.137	1.127	1.106	1.096	1.089
	1.151	1.126	1.101	1.112	1.111

with small sample masses have a somewhat larger error. Negative crosstalk does not represent a realistic quantity.

5.2 Cell constant

The cell constant gives the appropriate conversion factor of the

$$\text{Cell constant} = \Delta H_{\text{standard}} / \Delta H_{\text{measured}} \tag{4}$$

Table 4 shows the effect of heating rate and sample weight on the cell constant. It is almost constant for both cells when a heating rate of 5-20/min and indium weight of 5-20 mg are used. Similarly, the difference between the cells is small.

5.3 Temperature lag

A typical melting curve of indium is shown in Fig 6. One distinguishes the onset temperature, T_{o}, at the extrapolation of the linear position of the leading edge of the melting peak to the baseline and the initial temperature, T_{i}, at the extrapolation to the isotherm.

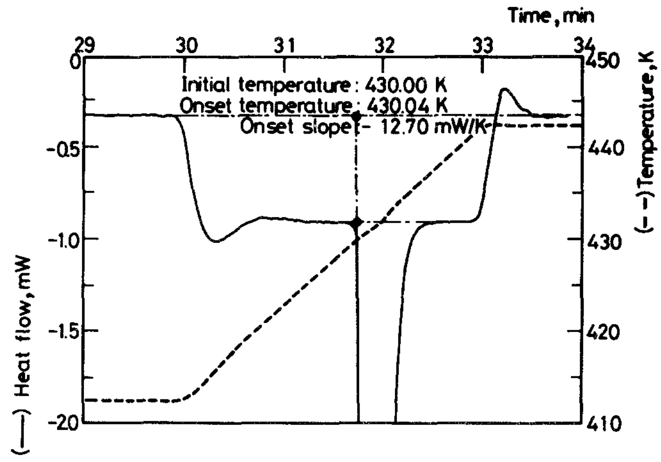

Fig. 6 A typical melting curve of indium

The difference between T_{o} and T_{i} is small, but both T_{o} and T_{i} change with heating rate and sample mass, as is shown in Figs 7 and 8. The sample mass effect can be expressed in terms of the heat flow amplitude A. For the heat-

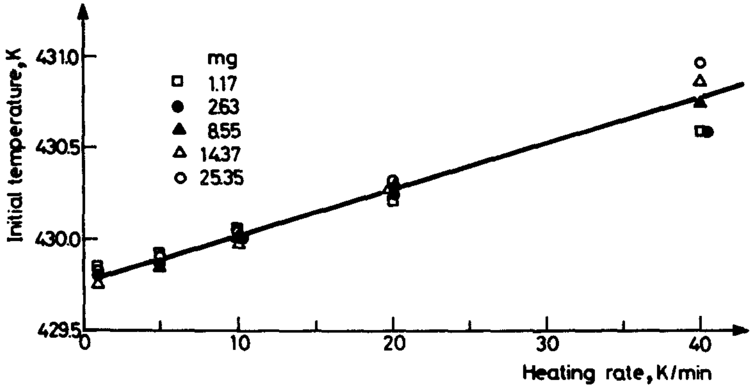

Fig. 7 Effect of heating rate on initial temperature with different indium mass for cell A

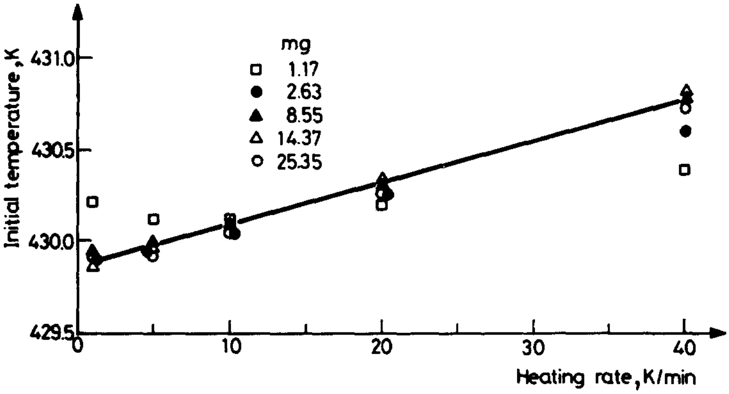

Fig. 8 Effect of heating rate on the initial temperature, Ti, with different indium masses for cell B

ing rates between 5 and 20 deg/min and indium masses of 5-20 mg the onset slope of a plot of *A* as a function of heating rate was 11.5 ±0.5 mW/deg for cell *A* and 12.5 ±0.1 mW/deg for cell *B*. The combined temperature lag ΔT is thus:

$$\Delta T = q/40 + A/12 \qquad (5)$$

where q is the heating rate in deg/min and A is the heat flow amplitude in mW. The corrected temperature is thus:

$$T_{\text{corrected}} = T_{\text{measured}} - \Delta T \qquad (6)$$

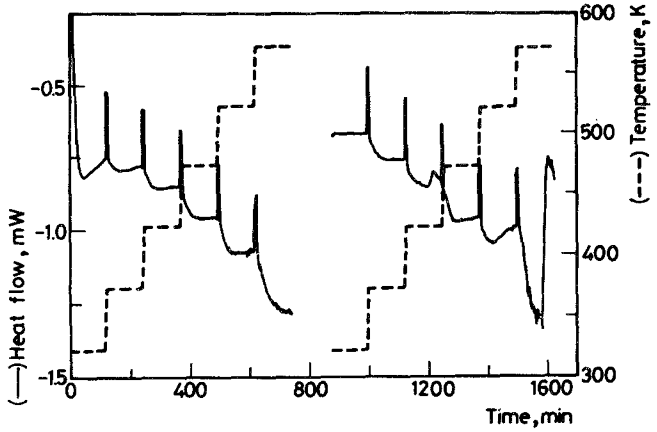

Fig. 9 Effect of the environment on DSC curves. Shown is the isothermal baseline interrupted by 50 K steps of temperature increases at 10 deg/min. Time: 0 to 800 min 1:00 PM to 2:20 AM; 1200 min = 9:00 AM; run completed at 3:00 PM

6. *Effect of the environment*

Fluctuations of the temperature of the environment have a significant effect on the baseline quality. This becomes obvious when it was observed that night runs are better than daytime runs, as shown in Fig. 9. The runs represent stepwise increases in the temperature (at 10 deg/min) programmed between 1:00 PM to the next day 3:00 PM. The night runs are stable and more repeatable. The baseline shifts at 1200 minutes can be correlated with openings of doors and windows and even just opening the cover of the DSC instrument. The last major excursion of the baseline at about 1600 min was caused by turning-on a fan directed towards the DSC (jump of about 0.6 mW for cell *A* and 0.15 mW for cell *B*). The jacket heater of the Autosampler covers the DSC cell and keeps the temperature outside of the DSC cell at about 323 K. It reduces the effect of the environment by about 30%. This is not sufficient to exclude environmental effects. A temperature-controlled room with minimal fluctuations and a separate enclosure of the calorimeter is needed for high quality baseline performance.

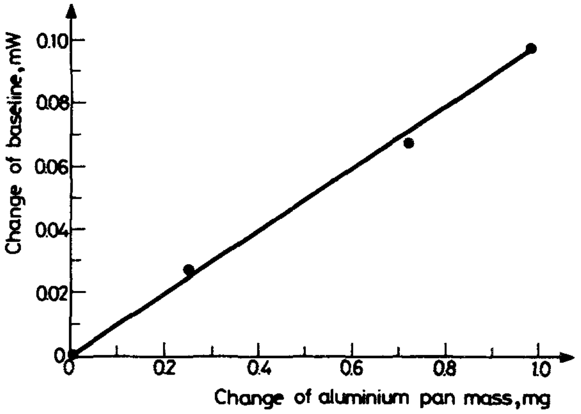

Fig. 10 Effect of the aluminium pan mass on baseline. Note that the slope is not related to the aluminium specific heat capacity

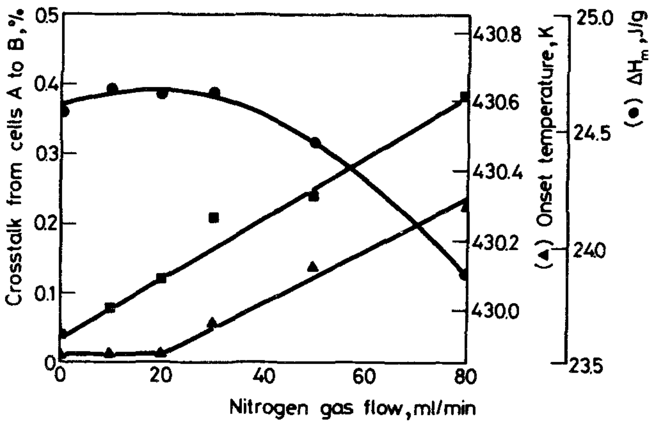

Fig. 11 Effect of nitrogen gas flow on the crosstalk (filled squares, left ordinate), the onset temperature (asterisks) and the heat of fusion of indium (filled circles)

7. Effect of the aluminum pan mass

For heating capacity measurement, it is important to have aluminum pans of similar masses [7]. The effect of the differences in pan mass on the baseline is shown in Fig. 10. Only if the pans on the calorimeter positions (A, B, R) have masses change within ±0.1 mg and the heat flow amplitude of the sample is 10 mW or more, will the error be within ±0.1%. In principle, the slope of the curve in Fig. 10 should be proportional to the specific heat capacity of aluminum. The calculated heat capacity of aluminum from the slope is, however, 30% lower than expected. It is thus best to select pans that have masses within ±0.1 mg and correct for the difference in aluminum mass by computation with the calibrated slope, if needed.

8. Effects of gas flow

In order to protect the sample from oxygen, nitrogen gas is passed through the DSC cell. This nitrogen gas flow affects the results significantly.

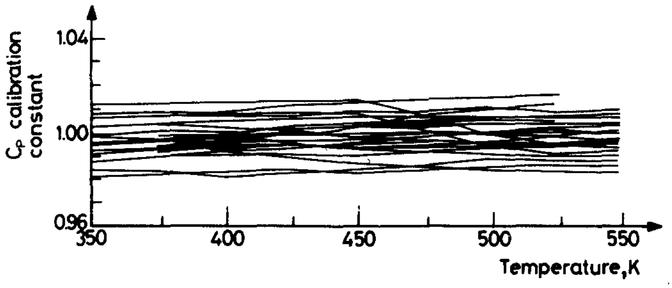

Fig. 12 Calibration constant of heat capacity as it varies over a long time period. Average and RMS: 0.997 ± 0.014

Figure 11 shows the effect of nitrogen gas flow on the onset temperature T_0 (asterisks), the heat of fusion of indium (filled circles), and the crosstalk from cell A to B (filled squares). It can be seen that both onset temperature and crosstalk change with increasing gas flow. For the crosstalk the percentage errors beyond 10 ml/min are all positive and ultimately take on the shape of clear melting peaks, rather than baseline noise. The nitrogen gas flow should be kept thus at about 10 ml/min, but no more than 20 ml/min. The results show clearly that increasing nitrogen flow changes the nature of the heat flux from conduction through the disk to (less reproducible) conduction through the turbulent gas flow.

9. Effect of heating rate differences between sample and reference

As discussed in the prior paper, the heat capacity in a triple-run DSC based on heat conduction can be expressed as follows [5]:

$$C_p = K\Delta T/q + [(K\Delta T/q + W)(\mathrm{d}\Delta T/\mathrm{d}T_S)] \tag{7}$$

where ΔT is the temperature difference between reference and sample (directly accessible from the DSC recording), T_S is the sample temperature, K is determined by comparison between sample and the calibration Al_2O_3 run, and q is the steady-state heating rate ($\mathrm{d}T_{\text{heater surface}}/\mathrm{d}t \approx \mathrm{d}T_{\text{reference}}/\mathrm{d}t$) and W is the heat capacity of the empty aluminum pan (water value). The term in brackets is small, but not directly recorded in standard DSC and thus usually neglected. It represented the deviation from steady-state in the sample calorimeter and is approximately the total heat capacity ($C_p + W$) multiplied with the slope of the DSC curve (ΔT *vs.* T_S). For a horizontal baseline (no change in steady state, $\mathrm{d}\Delta T/\mathrm{d}T_S = 0$) the heat capacity is exactly equal to $K\Delta T/q$, as usually assumed. Naturally, true baseline slopes, unchanged by electronic slope corrections are needed for the evaluation of $\mathrm{d}\Delta T/\mathrm{d}T_S$.

An effort was made to evaluate the magnitude of this correction term. Because the duPont DSC records only heat flow, the relationship between temperature difference (ΔT) and heat flow needed first to be established. In the DSC mode the signal can be displayed as original signal (mV) and as heat flow (mW) allowing the establishment of the relationship:

$$\text{Signal (mV)} = K' \times \text{heat flow (mW)} \tag{8}$$

The proportionality constant K' changes with temperature because of the non-linear thermocouple output. It could be fitted to the following equations:

$$\text{for cell } A\text{: } K'_A = 13.83695 + 6.295888 \times 10^{-3}\,T - 1.746529 \times 10^{-5}\,T^2 \tag{9}$$

$$\text{for cell } B\text{: } K'_B = 13.97081 + 5.751665 \times 10^{-3}\,T - 1.691952 \times 10^{-5}\,T^2 \tag{10}$$

In the DTA mode, the signal can be displayed in addition as original signal (mV) and temperature difference $\Delta T(K)$,

$$\text{Signal (mV)} = K'' \times \Delta T \tag{11}$$

we found K'', as expected, to be constant (19.994 ± 0.008). So, that the relationship between ΔT and heat flow (HF) is given by:

$$\Delta T = (K'/K'') \times \text{heat flow} = f(T) \times \text{heat flow} \tag{12}$$

For cell A:

$$f(T) = 0.6920551 + 3.148889 \times 10^{-4}\, T - 8.735266 \times 10^{-7}\, T^2 \tag{13}$$

and for cell B:

$$f(T) = 0.6987501 + 2.876696 \times 10^{-4}\, T - 8.462299 \times 10^{-7}\, T^2 \tag{14}$$

For both cells $\overline{f(T)} = 0.65 \pm 0.03$ from 348 to 548 K.

Table 5 Evaluation of $f(T)$ for sapphire[a)]

T_s, K	C_p (Al_2O_3), J/K mol	HF, mW	$K'(T)$, mV/mW	$f(T)$ K/mW	dHF/dT mW/K
348.15	88.5938	7.4658	13.9119	0.6958	–
373.15	92.5206	7.7405	13.7544	0.6879	0.0110
398.15	95.9321	8.0367	13.5750	0.6790	0.0118
423.15	98.9033	8.2733	13.3738	0.6689	0.0095
448.15	101.5118	8.5454	13.1508	0.6577	0.0109
473.15	103.8257	8.6884	12.9059	0.6455	0.0057
498.15	105.8990	8.8606	12.6392	0.6322	0.0069
523.15	107.7707	9.0660	12.3506	0.6177	0.0082
548.15	109.4676	9.2353	12.0403	0.6022	0.0068
		Averages:	13.0780	0.6541	0.0088

a)sapphire sample (62.8 mg) on cell A, heating rate: 10 deg/min, $d\Delta T/dT_S = f(T) \times (dHF/dT_S)$

An example data set for the sapphire standard is shown in Table 5. Column 2 is the heat capacity of sapphire. Column 3 is the recorded heat flow of the sapphire sample. Column 4 and 5 are $K'(T)$ and $f(T)$, respectively. From the slope of the heat flow *vs.* temperature curve (i.e. $dHF/dT = 0.00088$) one can estimate that $d\Delta T/dT_s$ is about 0.0057 (K/K). The term in brackets of Eq. (7) is thus about 0.5 to 1 % of C_p. If the sample and standard of similar amplitudes are run simultaneously by dual sample DSC or successively by triplerun DSC, a calibration with similar slopes would have similar deviations and largely compensate itself.

More precisely, for the single-run DSC, the heat capacity can be expressed as follows:

$$C_{pA} = K\Delta T_A / q + [(K\Delta T_A / q + W)(d\Delta T_A / dT_A)] \tag{15}$$

$$C_{pB} = K\Delta T_B / q + [(K\Delta T_B / q + W)(d\Delta T_B / dT_B)] \tag{16}$$

Assuming, as before, that the terms in brackets are small, one gets as a first approximation.

$$C_{pB} = C_{pA}(\Delta T_B / \Delta T_A) \tag{17}$$

The full expression for the heat capacity derived earlier is, however [5]:

$$C_{pB} = C_{pA} \times \frac{K\Delta T_B / q + [(K\Delta T_B / q + W)(d\Delta T_B / dT_B)]}{K\Delta T_A / q + [(K\Delta T_A / q + W)(d\Delta T_A / dT_A)]} \tag{18}$$

or on neglecting W:

$$C_{pB} = C_{pA} \times \frac{\Delta T_B (1 + d\Delta T_B / dT_B)}{\Delta T_A (1 + d\Delta T_A / dT_A)} \tag{19}$$

As an example, we measured a sapphire standard (62.38 mg) on cell A and an aluminum sample (80.14 mg) on cell B by DSDSC; the slopes of heat flow *vs.* temperature curves are 0.0088 and 0.0038 mW/K, respectively.

$$C_{pB} = C_{pA} \times \frac{\Delta T_B (1 + 0.65 \times 0.0038)}{\Delta T_A (1 + 0.65 \times 0.0088)} = 0.9968 \times C_{pA}(\Delta T_B / \Delta T_A) \tag{20}$$

i.e. with an approximately 50% difference in slope the remaining error is 0.3%. Obviously, this effect must be corrected for in precision heat capacity. If not, care must be taken to calibrate with approximately equal heat flow.

10. General discussion of the precision measurement

Most of the errors discussed up to now were of the order of magnitude of ±0.1% or could be controlled by careful measurement to within ±0.1%, except for the error caused by change of the temperature of the environment. The dual sample DSC has the advantage that it can run the standard and unknown sample at the same time, thus reducing the environmental effects somewhat. In addition, presence of the Autosampler with its constant temperature jacket reduces the effect of the environment temperature somewhat. By keeping environment effects controlled, the described errors should lead to an overall precision of perhaps ±0.3%. This figure was arrived at by taking the most probable value of the 10 errors, assuming each to have an approximate magnitude of ±0.1%.

All errors discussed are based on the assumption of a heat flow of 10 mW of the sample. To decrese the error even further, it would be best to increase the heat flow amplitude of the sample. There are two ways to accomplish that: First, one could increase the sample mass, but this route is limited by the sample density and pan size. The second way to increase the heating rate for increased sensitivity, but, the resolution and temperature accuracy will decrease in this case [8]. The experiments show that for both larger sample size and faster heating fluctuation of the amplitude increases. The decrease of the experiment error is thus relatively small. In addition, temperature lag and crosstalk become bigger. Overall we found that 10 deg/min to 20 deg/min with a standard sample pan filled to maximum capacity seems to be an optimum for heat capacity measurement.

B. Sample heat capacity measurements

With DSC adjusted for optimum conditions, the long-time baseline stability of the DSDSC was checked and the calibration established. This is followed by a discussion of data on five largely different samples.

1. Long-time baseline stability

It is necessary to know the baseline repeatability for heat capacity measurement by single-run DSDSC. We ran the experiments of the static baseline repeatability as shown in Figs 3 over a long period of time with the same run method unloading and loading and sample with the Autosampler.

After measuring the baselines of empty pans of over fifty runs over more than 10 weeks, the fluctuation of the corrected amplitude of the baseline was less than ±0.1 mW in the temperature range from 350 K to 550 K (independent of the fluctuation of the actual recorded amplitude of the baseline). This leads to a ±1% error if the amplitude of the sample is about 10 mW. This larger than expected fluctuation was caused mainly by the effects of the environment. By using automatic night-time runs, the error could be reduced to only ±0.1%. That means, as pointed out before, that thermal history or thermal environment is the most important factor in the repeatability.

2. Calibration constant of the heat capacity

Assuming the above dynamic baseline repeatability is sufficient for single-run DSC heat capacity measurement, we can measure the heat capacity of a sample, placed on cell B, based on the heat capacity of a standard sapphire sample, placed on cell A, by a single DSC run. The heat capacity of the sample can then be easily calculated by the approximate Eq. (1) for the case that symmetry exists between cells A and B.

We used two standards with almost the same mass of aluminum pan, cover and sapphire disk (one as the standard, the other as the unknown sample) to establish the difference of heat capacity between cells A and B. Measurements of this pair were repeated over 25 times over a long time period and it was found that the calibration constant for heat capacity was $K = 0.997 \pm 0.014$ from 350 to 550 K. The collective results are shown in Fig. 12.

Again, the ±1.5% fluctuation for the different runs is most probably caused by the change of the environment temperature during the different runs.

Heat capacities of five samples

Aluminum, sodium chloride, quartz, polystyrene and selenium were chosen to evaluate the instrument for the measurement of heat capacities. Table 6 shows the experimental heat capacities and error of the samples when compared with literature data [10-15]. The average error of all data is close to zero indicating no systematic error. The root mean square error of 0.8% is in line with the prior analysis and is quite acceptable for the evaluation of heat capacities and somewhat better than the triple run instrumentation [1, 3]. With control of the environment and inclusion of corrections for all lesser effects it should be possible to reach the ultimate goal of ±0.1% precision.

Table 6 Heat capacities of five samples

T,	Aluminium		Sodium chloride		Quartz		Polystyrene		Selenium	
K	C_p J/K mol	Error %	C_p J/K mol	Error, %	C_p J/K mol	Error, %	C_p J/K mol	Error, %	C_p J/K mol	Error, %
348.15	24.86	−0.50	51.39	−0.16	49.30	−0.30	151.78	0.58	25.89	0.58
373.15	24.98	−1.22	52.16	0.49	51.75	0.91	Glass transition		26.11	0.25
398.15	25.20	−1.60	52.29	−0.06	53.15	0.20	196.66	−2.08	26.33	−0.07
423.15	25.93	0.09	53.16	0.81	55.18	0.77	203.88	−1.72	26.50	−0.53
448.15	26.18	−0.16	53.56	0.79	56.94	0.90	213.22	−0.37	26.79	−0.58
473.15	26.55	0.06	53.59	0.11	57.77	−0.46	222.48	0.82	27.26	0.03
498.15	26.96	0.44	54.20	0.53	59.42	−0.26	228.96	0.74	Melting	
523.15	27.15	0.02	54.66	0.70	61.02	0.01	236.95	1.28	35.03	−0.55
548.15	27.49	0.12	54.87	0.40	61.47	−1.40	241.89	0.56	34.52	−1.17

*Error (%) = (1−expt. C_p /lit. C_p) x 100 %
Avarage and RMS error = −0.02 ±0.78 %
Heating rate : 10 deg/min, gas flow rate : 10 ml/min

Further work towards such improvements is in progress and expansion to the low temperature region is planned.

* * *

This work was supported by the National Science Foundation, Polymer Program Grant # DMR 8818412 and the Division of Materials Sciences, Office of Basic Energy Sciences, U.S. Department of Energy, under Contract DE-AC05-84OR21400 with Martin Marietta Systems, Inc. In addition, support by the duPont Company in acquisition of the instrumentation is acknowledged.

References

1 A. Mehta, R. C. Bopp, U. Gaur and B. Wunderlich J. Thermal Anal., 13 (1987) 197.
2 B. Wunderlich and U. Gaur, ACS Adv. in Chemistry Series 203, C. D. Craver, ed. Washington DC, pg. 195, 1982.
3 U. Gaur, a. Mehta and B. Wunderlich, J. Thermal Anal. 13 (1978) 71; A. Mahta and B. Wunderlich, Coatings and Plastics Preprints, Am. Chem. Soc., 35 (2) (1975) 393.
4 S. F. Lau and B. Wunderlich, J. Thermal Anal., 28 (1983) 59.
5 B. Wunderlich, J. Thermal Anal., 32 (1987) 1949.
6 duPont Instruments, Textbook of Thermal Analysis Users Training Course, Wilmington, DE, 1989.
7 H. Suzuki and B. Wunderlich, J. Thermal Anal., 29 (1984) 1369.
8 W. W. Wendlandt, Thermal Analysis, 3rd ed., John Wiley & Sons, New York, 1986.
9 D. C. Ginnings and G. T. Furukawa, J. Am. Chem. Soc., 75 (1953) 522.
10 M. W. Chase, Jr., C. A. Davies, J. R. Downey, Jr., D. J. Frurip, R. A. McDonald, and A. N. Syverud, "JANAF Thermochemical Tables" 3rd Ed., in J. Phys. Chem. Data, Vol. 14, Suppl. 1, 1985.
11 O. Kubaschewski and E. LL. Evans, Metallurgical Thermochemistry Pergamon Press, New York, 1958.
12 U. Gaur and B. Wunderlich, J. Phys. Chem. Ref. Data, 11 (1982) 313.
13 U. Gaur, H. C. Shu, A. Mehta and B. Wunderlich, ibid, 10 (1981) 89.
14 H. Von Moser, Physik. Zeitschr., 37 (1936) 747.
15 I. Barin and O. Knacke, "Thermochemical Properties of Inorganic Substances" Springer-Verlag, New York, 1973.

Zusammenfassung — Es wird eine Untersuchung eines single-run DSC vorgestellt, die fogendes berücksichtigt: Grundlinienreproduzierbarkeit, crosstalk zwischen Kalorimetern, Einstellung von Kalorimetern, Aufheizgeschwindigkeit, Probenmasse, Umweltver änderungen, Probenhaltermasse, Spülgasfluss, Instrumentträgheit und Unterschiede in der Aufheizgeschwindigkeit der Kalorimeter. Das fragliche Instrument war ein duPont Doppelproben DS-Kalorimeter. Die grössten Fehler werden durch Umwelteinflüsse verursacht. Alle anderen Fehler scheinen die Genauigkeit auf das akzeptierbare Mass von ±0.3% zu begrenzen. Nach einer Optimierung aller Parameter wurden bei Temperaturen zwischen 348 und 548 K die Wärmekapazitäten von Aluminium, Natriumchlorid, Quarz, Polystyrol, und Selen gemessen. Die Standardabweichung aller Messungen im Vergleich mit der relativ gut bekannten adiabatischen Kalorimetrie beträgt ±0.8%. Dies beweist, dass die single-run DSC, wie schon darauf hingewiesen, prinzipiell möglich ist, Verbesserungen aber noch möglich sind.